SINGLE AND MULTIPHONON RESONANCES AT ZERO AND FINITE TEMPERATURES WITHIN THE PHONON DAMPING MODEL

NGUYEN DINH DANG
1) RI-Beam Factory Project Office, RIKEN, 2-1 Hirosawa, Wako
351-0198 Saitama, Japan
2) Institute for Nuclear Science and Technique
Vietnam Atomic Energy Commission, Hanoi - Vietnam

Abstract

The application of phonon damping model is discussed to describe i) the giant dipole resonance (GDR) in hot nuclei, ii) multiple-phonon resonances, and iii) GDR in neutron-rich nuclei. The results are compared with recent experimental data and predictions of other theories.

The observed width of the giant dipole resonance (GDR) in highly excited (hot) nuclei increases with excitation energy E^* up to $E^* \sim 130$ MeV in tin isotopes[1], and saturates at higher E^* [2]. An adequate theoretical model should describe correctly not only the width, but also the shape of the GDR as a function of excitation energy E^* (or temperature T). For the double GDR (DGDR), the experimental cross section of the Coulomb excitation is significantly larger (by ~ 33 – 78%) than that given by the harmonic picture, in which an n-phonon resonance is built from n non-interacting single-phonon resonances[3]. It is not clear if anharmonicities are the main reason for this discrepancy. In neutron-rich nuclei, the neutron excess leads to the appearance of the pigmy GDR. The question of the effect of GDR damping on the strength of the pigmy resonances still remains open.

The phonon damping model (PDM)[4,5] was proposed primarily to describe the damping of the hot GDR. In the PDM the mechanism that causes the sharp increase of the GDR width at low temperatures, $T \leq 3$ MeV, and its saturation at high temperatures, $T > 3$ – 4 MeV, is the coupling of GDR phonon to particle-particle and hole-hole configurations, which appear due to the deformation of the Fermi surface at $T \neq 0$. In this talk, the results of application of PDM in the description of hot GDR, double-, triple-GDRs (DGDR and TGDR), and GDR in neutron rich nuclei are presented in comparison with recent experimental data and other theories. The formalism of PDM applied to hot GDR, multiphonon GDRs, GDR in neutron-rich nuclei are given in detail in Refs. [4,5,6,12], respectively. The details of calculations of electromagnetic (EM) cross section of DGDR are given in [7]. The selection of PDM parameters is given in [4].

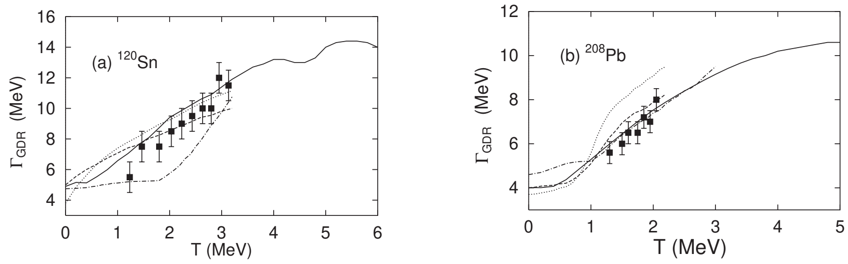

Figure 1: GDR width in ^{120}Sn (a) and ^{208}Pb (b) as a function of temperature T. Solid lines are PDM results; dashed lines: TFM results; dotted: PSM results; dash-dotted lines: CDM results. Inelastic α scattering data are from [1].

The solid lines in Fig. 1 are the GDR widths in ^{120}Sn and ^{208}Pb obtained within PDM. A clear saturation of $\Gamma_{\rm GDR}$ is seen at $T \geq 4$ MeV. The PDM results are found in better agreement with the data than those given by thermal fluctuations model (TFM), phenomenological scaling model (PSM), or collisional damping model (CDM) (See [8] and references therein). All the TFM, PSM, and CDM do not give a width saturation at $T > 3$ MeV.

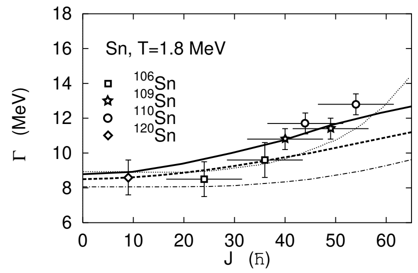

Figure 2: GDR widths as a function of angular momentum J. Results at $T = 1.8$ MeV within PDM are shown as dashed line for ^{120}Sn, and solid line for ^{106}Sn. The corresponding results within TFM are shown as dash-dotted and dotted lines, respectively. Data are from [1,9].

Shown in Fig. 2 are the GDR widths for ^{106,120}Sn obtained within PDM at $T = 1.8$ MeV as a function of angular momentum J in comparison with the data[1,9] and the prediction of TFM[9]. The angular-momentum effect is included in PDM by introducing an effective temperature $\widetilde{T} = \sqrt{T^2 + J(J+1)/(2a\mathcal{J})}$ ($\mathcal{J}$ is moment of inertia; $a = A/8$). Compared to the TFM, the PDM gives a stronger increase of width as a function of J up to $J \sim 55\ \hbar$. However, the overall increase of the GDR width with J is still rather weak.

The overall GDR shapes at different excitation energies are reproduced reasonably well using the PDM strength functions in the CASCADE calculations[10] as shown in Fig. 3. Inclusion of pairing at $T < 1$ MeV (solid curves)

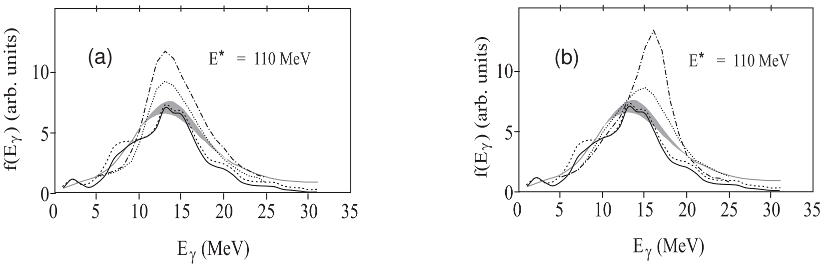

Figure 3: Experimental (shaded area) and theoretical divided spectra of GDR in ^{120}Sn at $E^* = 110$ MeV calculated within CASCADE using the strength functions of PDM (solid: including pairing, dashed: without pairing). Also shown in (a) are results obtained using strength functions of TFM with 100% of EWSR (dash-dotted) and 80% of EWSR (dotted) exhausted, and in (b) are those obtained using strength functions of CDM with free (dotted) and in-medium (dash-dotted) nucleon-nucleon scattering cross section [11].

Table 1: Energies $E_{\rm i}$, FWHM $\Gamma_{\rm i}$, and EM cross section $\sigma_{\rm C}^{\rm i}$ for GDR (i=GDR) (a) and DGDR (i=DGDR) (b), calculated within PDM (Theory) [7] in comparison with the experimental data (Experiment) [3] for ^{136}Xe and ^{208}Pb

a	$E_{\rm GDR}$ (MeV)		$\Gamma_{\rm GDR}$ (MeV)		$\sigma_{\rm C}^{\rm GDR}$ (mb)	
Nucleus	Theory	Experiment	Theory	Experiment	Theory	Experiment
^{136}Xe	15.6	15.2	4.96	4.8	1676.28	1420(42)±100
^{208}Pb	13.5	13.4	4.04	4.0	3039.67	3280±50
b	$E_{\rm DGDR}$ (MeV)		$\Gamma_{\rm DGDR}$ (MeV)		$\sigma_{\rm C}^{\rm DGDR}$ (mb)	
Nucleus	Theory	Experiment	Theory	Experiment	Theory	Experiment
^{136}Xe	29.2	28.3 ±0.7	7.0	6.3 ±1.6	159.33	164(85)±35
^{208}Pb	26.6	26.6 ±0.8	6.3	6.3 ±1.3	420.92	380 ±40

improves significantly the agreement with the data, especially at low E^*. The results obtained with the strength functions of TFM and CDM underestimate the GDR shape at low E^* (not shown) and overestimate it at high E^* [11].

The peak energies $E_{\rm i}$, FWHM $\Gamma_{\rm i}$, and EM cross section $\sigma_{\rm C}^{\rm i}$ for GDR and DGDR calculated within PDM for ^{136}Xe and ^{208}Pb [7] are shown in Table 1. They are in good agreement with the corresponding experimental data [3]. A systematic comparison between the results for DGDR and TGDR with anharmonicity and the results obtained by folding two and three GDRs predicts that the TGDR looks more harmonic than the DGDR [6].

Fig. 4 shows the strength functions of the GDR within PDM for ^{60}Ca at various T [12]. The pigmy resonance is clearly seen below 10 MeV at $T = 0$. It exhausts up to 5% (below 10 MeV) of the EWSR of the GDR (in ^{150}Sn). This pigmy resonance is smoothed out with increasing temperature.

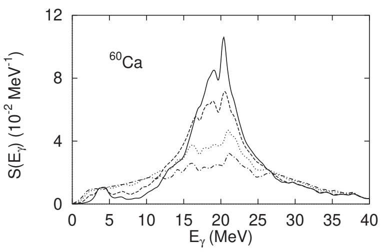

Figure 4: GDR strength functions in ^{60}Ca at $T = 0$ (solid), 1 (dashed), 2 (dotted), and 3 (dash-dotted) MeV.

In conclusion, the PDM is the only model up-to-date which has resolved simultaneously the experimental puzzles in the temperature and spin dependences of the hot GDR width and shape, in the EM cross sections of the DGDR in ^{136}Xe and ^{208}Pb, and can be applied to study the pigmy GDR in neutron-rich nuclei. The comparison with other theories shows that the results of PDM agree consistently better with the data for all of hot GDR characteristics in a wide range of temperatures up to $T \sim 6$ MeV. It is also the first time theory can describe simultaneously the EM cross sections of both GDR and DGDR.

References

1. T. Baumann et al., Nucl. Phys. A 635 (1998) 428.
2. P. Piattelli et al., Nucl. Phys. A 599 (1996) 63c.
3. K. Boretzky et al., Phys. Lett. B 384 (1996) 30; talk at the workshop on "Double giant resonance", Trento, May 10 - 22, 1999, unpublished.
4. N. Dinh Dang and A. Arima, Nucl. Phys. A 636 (1998) 443.
5. N. Dinh Dang, K. Tanabe, and A. Arima, Nucl. Phys. A 645 (1999) 536.
6. N. Dinh Dang, K. Tanabe, and A. Arima, Nucl. Phys. A 675 (2000) 531.
7. N. Dinh Dang, V. Kim Au, and A. Arima, to appear in Phys. Rev. Lett. (2000).
8. D. Kusnezov, Y. Alhassid, and K.A. Snover, Phys. Rev. Lett. 81 (1998) 542.
9. A. Bracco et al., Phys. Rev. Lett. 74 (1995) 3748; M. Matiuzzi et al., Nucl. Phys. A 612 (1997) 262.
10. N. Dinh Dang et al., Phys. Rev. C 61 (2000) 027302.
11. G. Gervais, M. Thoennessen and W.E. Ormand, Phys. Rev. C 58 (1998) R1377.
12. N. Dinh Dang, T. Suzuki, and A. Arima, Phys. Rev. C 61 (2000) 064304.